PERFORMANCE OF ADAPTIVE CODED MODULATION ENABLED BY LONG-RANGE FADING PREDICTION WITH DATA-AIDED NOISE REDUCTION

[*]Tao Jia, [*]Alexandra Duel-Hallen and [+]Hans Hallen
Department of [*]Electrical and Computer Engineering, [+]Physics
North Carolina State University
Raleigh, NC 27695, U. S. A.
Email: {tjia, sasha, hans_hallen}@ncsu.edu

ABSTRACT

Performance of uncoded adaptive modulation (UAM) and adaptive coded modulation (ACM) enabled by the long-range prediction (LRP) that utilizes data-aided noise reduction (DANR) is investigated for rapidly varying mobile radio channels. Due to improved prediction accuracy and low pilot rate, the DANR-aided LRP outperforms previously proposed prediction methods that rely on oversampled pilots to achieve noise reduction (NR). While ACM is more sensitive to prediction errors than UAM, utilization of DANR substantially increases its spectral efficiency (SE) relative to previously proposed methods. The set of SNR values and prediction ranges where positive coding gain is achieved by ACM enabled by DANR-aided LRP is determined. It is also demonstrated that adaptive modulation (AM) aided by LRP has better performance for the realistic physical model than for the Jakes model in the practical SNR range.

I. INTRODUCTION

Adaptive modulation (AM) has been proposed to improve the spectral efficiency (SE) for fading channels [1]. The uncoded adaptive modulation (UAM) schemes that employ multilevel quadrature amplitude modulation (MQAM) were investigated in [1, 2]. To improve SE, the adaptive coded modulation (ACM), also known as adaptive trellis-coded modulation (TCM), was proposed [3,4,5,6,7]. When reliable channel state information (CSI) is available, the ACM achieves significant coding gain over the UAM [3]. On the other hand, it has been shown that this coding gain diminishes when the CSI becomes unreliable [6, 7]. When the CSI is very inaccurate, UAM outperforms ACM.

To maintain the CSI accuracy and, therefore, SE of adaptive transmission methods in rapidly varying mobile radio channels, fading prediction is required [8]. We employ the long-range prediction (LRP) method, which was shown to achieve superior performance for realistic channel models and measured channels [8, 9,10,11]. For practical signal-to-noise ratio (SNR) values, noise reduction (NR) is required for the LRP. Methods that rely on oversampled pilots were proposed to achieve NR [11, 12]. However, the SE of these high-rate pilot techniques methods is significantly degraded due to resources consumed by transmitting pilot symbols [13].

To improve the prediction accuracy while maintaining the SE, a novel data-aided noise reduction (DANR) method was proposed in [13] for UAM. In this method, MQAM symbols are coherently detected using low-rate pilot symbols as well as predicted future channel coefficients. These decisions are employed to obtain improved channel estimates. Due to high data rate of these decisions, NR is achieved without utilizing oversampled pilots. Then the improved channel estimates are passed through a robust filter that suppresses out-of-band noise, and decimated to obtain low-rate channel estimates used for LRP. It was demonstrated in [13] that the DANR technique outperforms existing pilot-based methods in terms of both prediction accuracy and SE for UAM systems.

In this paper, we investigate the application of DANR to ACM systems. To obtain timely improved channel estimates for LRP, the decoded MQAM symbols are employed. The effect of reduced traceback depth for recently observed symbols on the prediction accuracy is investigated. The SE gain of DANR relative to pilot-aided NR methods is quantified for ACM. Moreover, we find the set of channel conditions where the ACM achieves coding gain relative to the UAM when DANR is employed. Thus, the values of SNR and prediction ranges where coding is beneficial are determined. The standard Jakes model and our realistic physical model are employed in testing the proposed methods.

The remainder of this paper is organized as following. UAM and ACM enabled by LRP are discussed in section II. The proposed DANR method for ACM is described in

This research was supported by ARO grant W911NF-05-1-0311

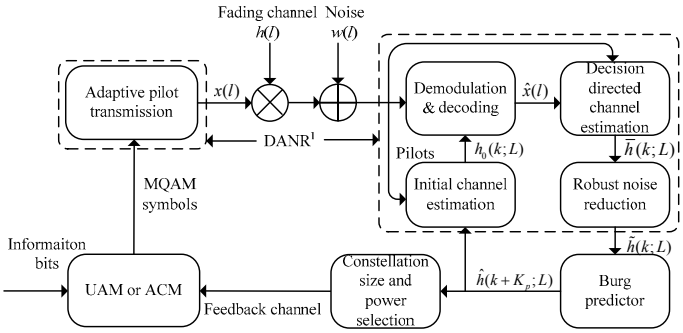

Fig. 1. System diagram.

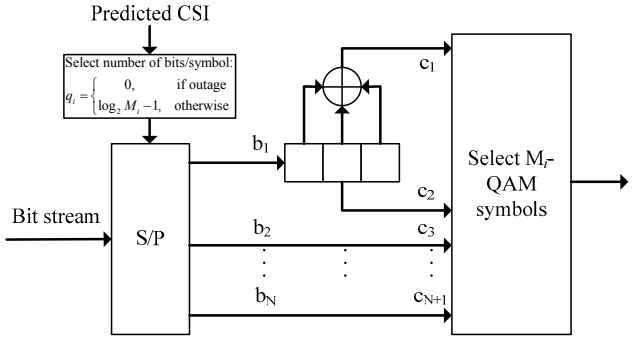

Fig. 2. Adaptive coded modulation (ACM) scheme employed in this paper.

Table I. Notation

f_{dm}	Maximum Doppler frequency
f_s	Symbol rate
f_p	Sampling rate of predictor
$h(l)$	Channel coefficient of the lth symbol
$h(k;L)$	Channel coefficient of the kth frame
L	Frame size
K	Superframe size
J	Decimation factor after robust filtering
P_{pred}	Order of prediction filter
E_p	Pilot symbol energy
E_s	Average energy of all symbols
λ	Carrier wavelength

section III. Finally, numerical results and conclusions are presented in sections IV and V, respectively.

II. ADAPTIVE MODULATION AIDED BY LONG-RANGE PREDICTION

Consider the system diagram illustrated in Fig. 1 [13]. The equivalent lowpass received lth sample is

$$y(l)=x(l)h(l)+w(l), \tag{1}$$

where $x(l)$, $h(l)$, and $w(l)$ are the transmitted symbol, the complex flat Rayleigh fading channel coefficient with $\mathrm{E}[|h(l)|^2]=1$, and complex white Gaussian noise with variance N_0, respectively. The transmitted symbols can be either pilots or data symbols. Without loss of generality, we assume that $x(l)=\sqrt{E_p}$ when pilots are transmitted. Frequently used notation of this paper is summarized in Table I.

To enable AM, the fading coefficient is predicted using a linear predictor (LP) [8]. The actual fading coefficient $h(l)$ and its prediction $\hat{h}(l)$ are jointly Gaussian random variables with the cross-correlation [7, 13]

$$\rho \triangleq \mathrm{E}[h(l)\hat{h}^*(l)]/\sigma_{\hat{h}} \tag{2}$$

where $\sigma_{\hat{h}}^2=\mathrm{E}[|\hat{h}(l)|^2]$. In this paper, the *normalized prediction MSE* defined as $\mathrm{NPMSE}\triangleq 1-\rho^2$ is employed as an appropriate indicator of SE in AM aided by fading prediction [13]. Without loss of generality, we omit the time index l, and denote $\gamma=|h|^2$ and $\hat{\gamma}=|\hat{h}|^2$ in this section.

Consider a coded or uncoded AM system with constant power allocation [2, 13, 14], MQAM constellation sizes $M_i\in\{4, 16, 64, 256\}$, $i\in[1,\ldots,4]$, and switching thresholds γ_i, $i\in[0,\ldots,5]$, where $\gamma_0=0$ and $\gamma_5=\infty$. Fig. 2 illustrates our ACM scheme that employs a simple rate 1/2 convolutional encoder with four states [3]. It was shown in [3] that this ACM scheme achieves approximately 3dB power gain relative to the UAM when the CSI is perfect. If M_i-QAM is selected ($i>0$), two coded bits and $\log_2 M_i-2$ uncoded bits are mapped to an M_i-QAM symbol.

Given fixed average $\mathrm{SNR}=E_s/N_0$, where E_s is the average overall symbol energy that includes energy of both data and pilot symbols, the calculation of average MQAM data symbol energy E_d depends on the pilot transmission scheme. We employ pilot-based LRP methods where the pilot energy E_p is equal to the average symbol energy, i.e., $E_p=E_s$. Thus, $E_s=E_d\int_{\gamma_1}^{\infty} p(\hat{\gamma})d\hat{\gamma}=E_d\exp\left[-\gamma_1/\sigma_{\hat{h}}^2\right]$ [2, 13], where $p(x)$ is the probability density function of a random variable x. When the SE loss caused by transmitting pilots is not taken into account, the SE is evaluated as

$$S_d=\sum_{i=1}^{4}\left[\log_2(M_i-1)\int_{\gamma_i}^{\gamma_{i+1}}p(\hat{\gamma})d\hat{\gamma}\right]. \quad (3)$$

We employ the UAM method described in [2, 11], and the ACM scheme based on the design in [6]. Given the reliability of prediction ρ (2), these methods select thresholds to maximize the SE while maintaining the average BER below the target BER P_t [2, 6]. Fig. 3 shows the SE of these systems S_d [2,6] for the target BER $P_t=10^{-4}$ and several average SNR levels when the SE degradation due to pilots is not taken into account. For the NPMSE on the order of 10^{-2} or smaller, prediction is sufficiently reliable to maintain near-optimal bit rate, and the SEs of both UAM and ACM are not sensitive to the variation of the NPMSE. On the other hand, these SEs decrease rapidly as the NPMSE approaches 10^{-1}, and the rate of decrease is greater for ACM than for UAM. This observation confirms the conclusion in [6,7] that ACM is more sensitive to the prediction errors than UAM. For the NPMSE$\approx10^{-2}$, ACM has about 0.4 bps/Hz coding gain over the UAM, while UAM outperforms ACM when the NPMSE approaches 10^{-1}, which is often the case for realistic SNR values in practical mobile radio scenario [8, 9]. Therefore, to achieve positive coding gain in practical systems, the NPMSE should be decreased by employing NR.

Sensitivity of ACM to prediction errors was investigated in [6], and can be explained intuitively as follows. When prediction is unreliable, the BER of M_i-QAM for the AWGN channel at low SNR dominates the calculation of thresholds [2, 6] and results in reduced SE. Since TCM has higher BER than uncoded MQAM given the same bits/symbol in the AWGN channel with low SNR [1], UAM outperforms ACM as the prediction accuracy decreases.

While the comparison in Fig. 3 is limited to a simple four-state encoder, it can be generalized for more complex encoders as follows. Increasing the number of states improves the coding gain for medium to high SNR, but degrades the BER at low SNR for the AWGN channel [3]. Therefore, the sensitivity of ACM to prediction errors increases as the number of states grows. This conclusion was confirmed by simulations that compared four-state and eight-state encoders in [7]. Thus, the benefit of NR is expected to increase with the number of states in the encoder.

III. DATA-AIDED NOISE REDUCTION FOR AM AIDED BY LRP

The frame structure of LRP aided by DANR was described in [13, Fig. 3]. The transmitted symbols are grouped into frames with L symbols where $f_s/L=100f_{dm}$, and the constellation size is fixed in each frame [13]. Since channel coefficient is approximately constant in frame k, it is denoted $h(k;L)\approx h(kL-l)$, $l\in[0,\ldots,L-1]$. K consecutive frames are grouped into a superframe, and one superframe pilot is transmitted at the end of each superframe [13]. Moreover, one pilot symbol is transmitted at the end of each frame that experiences outage. This method is referred to as adaptive pilot transmission.

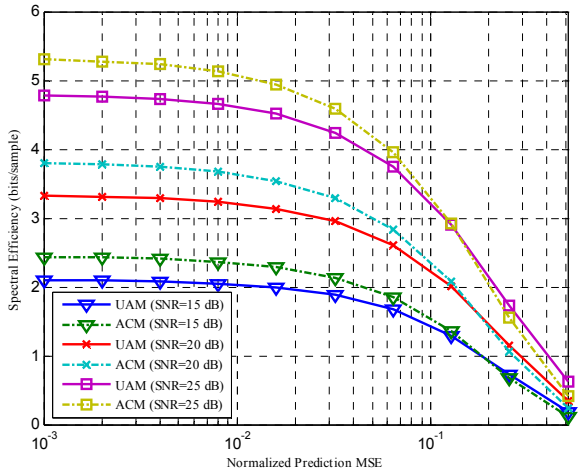

Fig. 3. Spectral efficiency of AM vs. NPMSE for target BER $P_t=10^{-4}$.

Let η denote the fraction of bandwidth dedicated to superframe pilots. The actual average SE of the system is $\overline{S}=(1-\eta)S_d$ bps/Hz, where S_d is given in (3). As discussed in [13], methods that rely on oversampled pilots to accomplish NR incur severe penalty in SE. In these systems the pilot rate is on the order of $100f_{dm}$, or $\eta=1/K$ [11], i.e., the frame rate in DANR, while the pilot rate $\eta=1/KL$ in DANR [13]. Note that pilots adaptively transmitted during outage frames in our adaptive pilot transmission method do not incur SE penalty since data symbols are not transmitted in those frames.

The power loss caused by transmitting pilots in adaptive pilot transmission also affects system performance. We select $E_s=E_p$ as in a pilot symbol assisted modulation (PSAM) system [15]. Although higher SE is achieved by optimally allocating power to data symbols and pilots as in [16], the SE loss of our method relative to the optimal allocation [16] is small due to the following reasons. First, the pilot symbols account for a small percentage of the available bandwidth. Therefore, reducing the power allocated to pilot symbols would not significantly improve the power allocated to the data symbols. Second, in DANR, the prediction accuracy mostly depends on the decision-directed data symbols [19]. Increasing the pilot

power by sacrificing data symbol power would not significantly improve the prediction accuracy provided the pilot SNR is maintained high enough to demodulate the received data symbols reliably. In addition, in our method, the selected pilot energy does not depend on the accuracy of prediction and is known at the transmitter while in the variable pilot energy method it depends on the NPMSE and needs to be fed back [16]. Thus, our method reduces the required feedback relative to the technique in [16].

In the proposed adaptive pilot transmission, M_i-QAM symbols ($M_i>0$) occupy $\frac{KL-1}{KL}\int_{\gamma_i}^{\gamma_{i+1}} p(\hat{\gamma})d\hat{\gamma}$ fraction of the bandwidth, and the pilots transmitted during outage frames that do not contain superframe pilots occur with probability $\frac{K-1}{KL}\int_{0}^{\gamma_1} p(\hat{\gamma})d\hat{\gamma}$. Therefore, the power constraint for our DANR method is given by

$$E_s=\frac{KL-1}{KL}E_d\int_{\gamma_1}^{\infty} p(\hat{\gamma})d\hat{\gamma}+\eta E_p+\frac{E_p}{KL}(K-1)\int_{0}^{\gamma_1} p(\hat{\gamma})d\hat{\gamma} \qquad (4)$$

This power constraint is used in the optimization of thresholds for AM.

As described in [13] for UAM, the initial channel estimates at the receiver are obtained by filtering the observed superframe pilots and one predicted future superframe pilot. These estimates are employed to demodulate the received data symbols coherently as follows. Suppose the initial channel estimate for the kth frame is denoted $h_0(k;L)$, and assume this frame is not an outage frame. In the ACM system, the soft input to the Viterbi decoder for symbol l (see (1)) is given by $y(l)/h_0(k;L)$, where $l\in[kL-L+1,\ldots, kL]$ are the indices of symbols in the kth frame. To reduce the BER of decisions used for the decision-directed NR, it is desirable to employ the decoded information bits. At time l_0, we select the survival path with the smallest metric, and use the information bits corresponding to this path as the decisions [17]. These decisions are re-encoded to obtain $\hat{x}(l,l_0)$, $l\le l_0$, the decision of symbols $x(l)$ at time l_0. The decoder traceback length is short for very recently observed data symbols, and they have high error rate. However, a traceback length of 5U (where U is the constraint length of the encoder) is sufficient for the decoding [18], and for the four-state encoder used in our system, the corresponding traceback length is only 15 information bits. This interval is much shorter than the memory span of the observation interval used for prediction [8]. Thus, the impact of increased decoding error rate on the performance of our DANR method is small.

The decisions $\hat{x}(l,l_0)$ are employed to improve the estimation of channel coefficient $h(k;L)$ at the frame rate. The estimation method is the same as for the UAM system [13]. Due to decision-directed estimation, the noise variance in these estimates $\bar{h}(k;L)$ is reduced by approximately a factor of L relative to the initial estimates $h_0(k;L)$ [13]. The estimates $\bar{h}(k;L)$ are passed through a robust NR filter to reject out-of-band noise and decimated by a factor of J samples to obtain estimates $\tilde{h}(n)$ with low sampling rate $f_p=f_s/(LJ)$. In our simulations, this low rate is given by the superframe rate, i.e., $J=K$.

The one-step prediction of channel coefficient is given by [8]

$$\hat{h}(n+1)=\sum_{p=0}^{P_{\text{Pred}}-1}\omega_{\text{pred}}^{*}(p)\tilde{h}(n-p), \qquad (5)$$

where P_{pred} is the order of predictor, and $\omega_{\text{pred}}(p)$, $p\in[0,\ldots,P_{\text{pred}}-1]$, are the coefficients of the predictor. The memory span of the predictor is defined as the time or spatial interval spanned by the samples used to perform one prediction, i.e., $\tilde{h}(n-p)$, $p\in[0,\ldots,P_{\text{pred}}-1]$. For this predictor, the memory span is $P_{pred}KL/f_s$ seconds, or $P_{pred}KLf_{dm}\lambda/f_s = P_{pred}K\lambda/100$, where λ is the carrier wavelength [9]. The Burg method is employed to estimate the predictor coefficients $\omega_{\text{pred}}(p)$ using an observation window that contains B past noise-reduced samples, where $B>>P_{\text{pred}}$. Finally, longer prediction ranges are achieved by iteration of (5) using the multi-step method [8].

IV. NUMERICAL RESULTS AND ANALYSIS

The standard Jakes model with nine oscillators as well as our realistic physical model is employed in simulations [8, 9]. The geometry of physical model data set used for testing LRP enabled by DANR is illustrated in [13, Fig. 4]. It represents a typical flat fading urban mobile radio channel with rms delay spread σ_d=1 us and f_{dm}=100 Hz. In all simulations, the symbol rate f_s= 100 Ksps, the frame size L=10, and K=10 frames per superframe are selected. The sampling frequency of the predictor is f_p=1 KHz=10f_{dm} and the order P_{pred}=20. The observation window of Burg predictor contains 200 and 100 samples for the Jakes and our practical physical models, respectively.

For comparison, we also simulated the performance of low-rate raw pilot and high-rate pilot methods with the pilot rates 10f_{dm} and 100f_{dm}, respectively [8, 11]. In the raw pilot method, Burg predictor is employed to predict future channel coefficients. The high-rate pilot method assumes

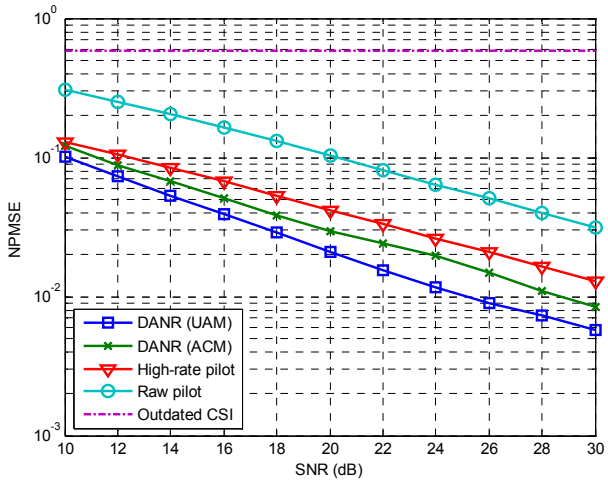

Fig. 4. NPMSE vs. SNR for prediction range 0.2λ in Jakes model.

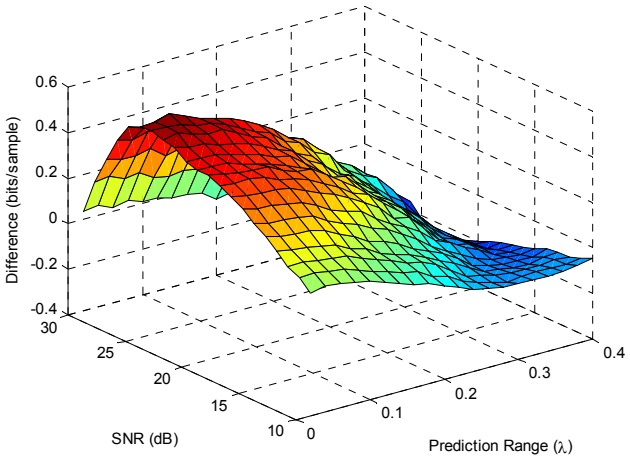

Fig. 6. Difference in SE between ACM and UAM with DANR.

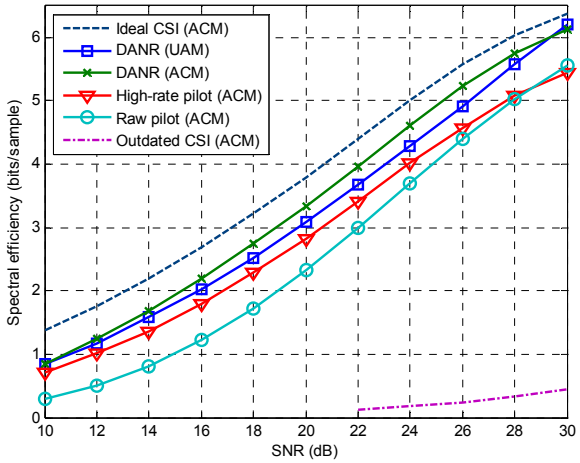

Fig. 5. SE vs. SNR for prediction range 0.2λ in Jakes model.

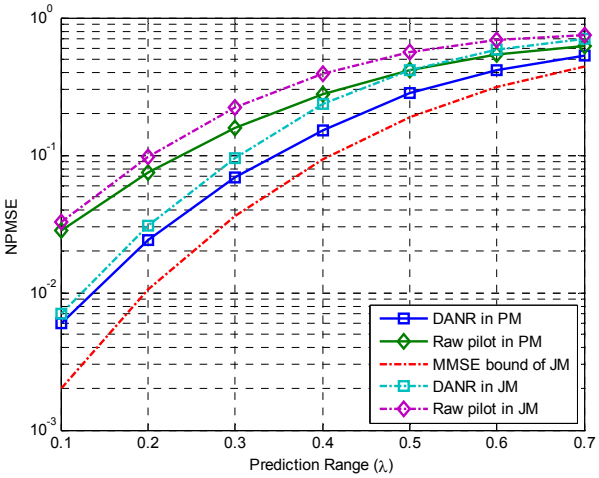

Fig. 7. NPMSE vs. prediction range for SNR=20dB, ACM, Jakes model (JM) or physical model (PM).

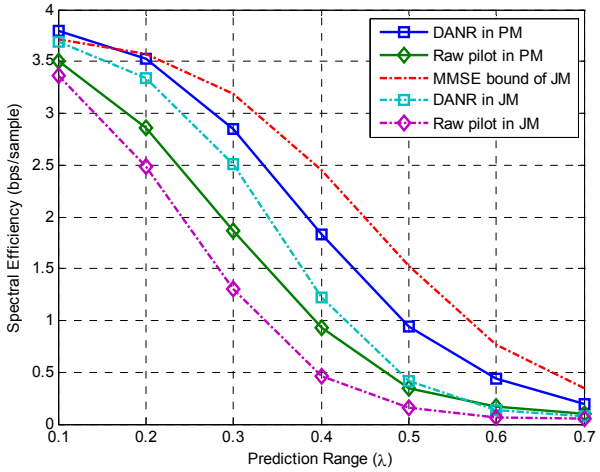

Fig. 8. SE vs. prediction range for SNR=20dB, ACM, Jakes model (JM) or physical model (PM).

the knowledge of channel statistics, and is employed only for the Jakes model in our paper. In this method, NR is performed using four filters with smoothing lags {0, 2, 5, 10} [11] and filter order 50. The outputs of these NR filters are down-sampled to a rate of f_p=10f_{dm} and then fed into the MMSE predictor. For fair comparison, the spatial memory span is given by 2λ for all prediction methods.

Fig. 4 and 5 illustrate the NPMSE and SE of several prediction methods for the Jakes model when the prediction range is 0.2λ. Due to accurate decisions of recently received data symbols, the DANR-aided prediction for UAM is more reliable than for ACM. However, since NR reduces the NPMSE below 10^{-1} for SNR≥10dB, the ACM achieves SE coding gain at low to medium SNR (see Fig. 3). At high SNR, the SE of ACM is limited by smaller maximum number of information bits

per symbol relative to UAM [6], since both AM methods employ the same set of constellation sizes. Therefore, UAM outperforms ACM when 256-QAM is frequently used at high SNR. Although the high-rate pilot method provides good prediction accuracy, its SE is smaller than for the DANR technique due to the penalty of transmitting oversampled pilots, and it has even lower SE than the raw-pilot method for high SNR. Similar conclusions were made in [13] for the UAM system enabled by the high-rate pilot method.

For the Jakes model, the SE gain of ACM over UAM is illustrated in Fig. 6 for different SNR and prediction ranges. Both systems are enabled by DANR-aided LRP. The maximum coding gain, 0.6 bits/sample, is achieved at SNR=24dB and the shortest prediction range (0.02λ). As the additive noise level and/or prediction range increase, the SE gap reduces due to less accurate prediction for the ACM system. To achieve a positive gain, the prediction range has to be less than 0.35λ.

In Fig. 7 and 8, the NPMSE and SE are shown versus prediction range for fixed SNR of 20 dB. Both the Jakes and physical models are employed in these simulations, and the SE gain of DANR over the raw pilot method approaches one bit/sample for each model. As discussed in [13], realistic physical model data sets are easier to predict than the Jakes model data at low to medium pilot SNR due to a small number and non-uniform distribution of reflectors, while the opposite conclusion holds for high pilot SNR where the non-stationarity of the physical model data causes performance degradation [9]. Thus, LRP-aided ACM has better performance for realistic physical model than for the Jakes model for the SNR=20dB investigated in Fig. 7 and 8.

The performance of the following "MMSE bound" predictor is also shown in these figures for the Jakes model. Suppose channel statistics are known, and consider a minimum mean square error (MMSE) predictor that employs pilots transmitted at the data rate. Let the memory span of this predictor be the same as for DANR-aided LRP. Thus, the corresponding filter order of this MMSE predictor is $P_{pred}KL$. Suppose this predictor enables an ACM scheme with parameters described in section II and bandwidth loss $\eta = 1/KL$. The resulting MMSE and SE of this MMSE predictor serve as lower and upper bounds on the achievable NPMSE and SE of our practical technique.

From Fig. 7, we observe that for shorter prediction ranges (≤0.2λ), the NPMSEs of the DANR and MMSE methods for the Jakes model do not significantly exceed 10^{-2}. When the prediction range increases to 0.4λ, the NPMSE of the DANR method grows over 10^{-1}, while it is below 10^{-1} for the MMSE bound. As illustrated in Figure 3, the SE is insensitive to the NPMSE values in the former case, but drops sharply for the latter case. Thus, the difference in SEs between DANR and the MMSE bound is small for shorter prediction ranges, and peaks at 1.2 bits/sample when the range is 0.4λ. The NPMSE degradation of the DANR-aided LRP relative to the MMSE bound predictor is due to several practical limitations, including decision errors, AR coefficient mismatch and robust NR filtering. Moreover, in the DANR method, decomposition of the prediction into three stages (decision-directed NR, robust filtering, and Burg predictor) results in simple but suboptimal solution relative to a single MMSE predictor with very large filter order. Note that a MMSE predictor that experiences outages at the same rate as in the LRP-aided AM system (i.e. utilizes adaptive pilot transmission where one pilot symbol is transmitted in each outage frame) has similar performance to our ideal MMSE predictor [19]. Thus, the impact of outages on the performance of DANR is small. This result is due to the utilization of adaptive pilot transmission that significantly improves performance of the DANR method [19].

V.CONCLUSIONS

The performance of coded and uncoded AM aided by long-range prediction is investigated. It is demonstrated that ACM is more sensitive to the prediction errors than UAM, and reliable prediction is required to achieve positive coding gain. The LRP aided by data-aided noise reduction (DANR) was proposed for ACM and shown to achieve much higher SE than previously investigated pilot-based methods due to its superior prediction accuracy and low pilot rate. The set of SNR values and prediction ranges where positive coding gain is achieved by ACM enabled by DANR-aided LRP was determined, and it was demonstrated that AM aided by LRP has better performance with the realistic physical model than for the Jakes model in the practical SNR range.

REFERENCES

[1] A. J. Goldsmith, and S.-G. Chua, "Variable-rate variable-power MQAM for fading channels," IEEE Trans. Commun., vol. 45, no. 10, pp. 1218-1230, Oct. 1997.

[2] S. Falahati, A. Svensson, T. Ekman and M. Sternad, "Adaptive modulation systems for predicted wireless channels," IEEE Trans. Commun., vol. 52, no. 2, pp. 307-316, Feb. 2004.

[3] A. J. Goldsmith, and S.-G. Chua, “Adaptive coded modulation for fading channels,” IEEE Trans. Commun., vol. 46, no. 5, pp. 595-602, May 1998.
[4] K. J. Hole, H. Holm, and G. E. Øien, “Adaptive multidimensional coded modulation over flat fading channels,” IEEE J. Selected Areas Commun., vol. 18, no. 7, pp. 1153-1158, July 2000.
[5] G. E. Øien, H. Holm, and K. J. Hole, “Impact of channel prediction on adaptive coded modulation performance in Rayleigh fading,” IEEE Trans. Veh. Technol., vol. 53, no. 3, pp. 758-769, May 2004.
[6] S. Falahati, M. Hong, A. Svensson, and M. Sternad, “Adaptive trellis-coded modulation over predicted flat fading channels,” Proc. IEEE VTC, 2003-fall, vol. 3, pp. 1532-1536.
[7] S. Zhou, and G. B. Giannakis, “Adaptive modulation for multiantenna transmissions with channel mean feedback,” IEEE Trans. Wireless Commun., vol. 3, no. 5, pp. 1626-1636, Sept. 2004.
[8] A. Duel-Hallen, Shengquan Hu and H. Hallen, “Long-range prediction of fading signals,” IEEE Signal Process. Mag., vol. 17, no. 3, pp. 62-75, May. 2000.
[9] A. Duel-Hallen, “Fading channel prediction for mobile radio adaptive transmission systems,” Proc. IEEE, vol. 95, no. 12, pp. 2299-2313, Dec. 2007.
[10] S. Semmelrodt and R. Kattenbach, "Investigation of different fading forecast schemes for flat fading radio channels," in Proc. IEEE VTC, 2003-Fall, pp. 149-153.
[11] T. Ekman, “Prediction of mobile radio channels: modeling and design,” Ph. D. Dissertation, Uppsala Univ., Sweden, 2002.
[12] K.E. Baddour, N. C. Beaulieu, “Improved pilot-assisted prediction of unknown time-selective Rayleigh channels,” Proc. IEEE Int. Conf. Commun., June 2006, vo. 11, pp. 5192-5199.
[13] T. Jia, A. Duel-Hallen, and H. Hallen, “Improved Long-Range Prediction with Data-Aided Noise Reduction for Adaptive Modulation Systems,” Proc. 43rd Annual Conference on Information Sciences and Systems, Princeton, NJ, 2008, available at: http://www4.ncsu.edu/~tjia/CISS2008.pdf.
[14] S. Zhou, G. B. Giannakis, “How accurate channel prediction needs to be for transmit-beamforming with adaptive modulation over Rayleigh MIMO channels?” IEEE Trans. Wireless Commun., vol. 3, no. 4, pp. 1285-1294, July 2004.
[15] J. K. Cavers, “An analysis of pilot symbol assisted modulation for Rayleigh fading channels,” IEEE Trans. Vech., vol. 40, no. 4, pp. 686-693, Nov. 1991.
[16] X. Cai and G. B. Giannakis, "Adaptive PSAM accounting for channel estimation and prediction errors," IEEE Trans. Wireless Commun., vol. 4, no. 1, pp. 246-256, Jan. 2005.
[17] R. Raheli, A. Polydoros and C. K. Tzou, "Per-survivor processing: a general approach to MLSE in uncertain environments, " IEEE Trans. Commun., vol. 43, pp.354-364, Feb.-Apr. 1995.
[18] J. Proakis, *Digital Communications*, 4th ed. New York, NY: McGraw-Hill, 2001.
[19] T. Jia, “Single and multicarrier adaptive transmission systems with long-range prediction aided by noise reduction”, Ph. D. Thesis, North Carolina State University, in preparation.